

# Global biodiversity patterns of marine forests of brown macroalgae

Eliza Fragkopoulou<sup>1</sup>  | Ester A. Serrão<sup>1</sup> | Olivier De Clerck<sup>2</sup> | Mark J. Costello<sup>3</sup> |  
 Miguel B. Araújo<sup>4,5</sup> | Carlos M. Duarte<sup>6,7</sup>  | Dorte Krause-Jensen<sup>6,8</sup> | Jorge Assis<sup>1</sup> 

<sup>1</sup>Algarve Center of Marine Sciences (CCMAR-Algarve), University of the Algarve, Faro, Portugal

<sup>2</sup>Phycology Research Group, Biology Department, Ghent University, Ghent, Belgium

<sup>3</sup>Faculty of Bioscience and Aquaculture, Nord Universitet, Postboks 1490, Bodø, Norway

<sup>4</sup>Department of Biogeography and Global Change, National Museum of Natural Sciences, CSIC, Calle José Gutiérrez Abascal, Madrid, Spain

<sup>5</sup>Rui Nabeiro Biodiversity Chair, MED – Mediterranean Institute for Agriculture, Environment and Development, University of Évora, Largo dos Colegiais, Évora, Portugal

<sup>6</sup>Arctic Research Centre (ARC), Aarhus University, Århus C, Denmark

<sup>7</sup>Red Sea Research Center (RSRC), King Abdullah University of Science and Technology (KAUST), Thuwal, Saudi Arabia

<sup>8</sup>Department of Bioscience, Aarhus University, Silkeborg, Denmark

## Correspondence

Eliza Fragkopoulou, Algarve Center of Marine Sciences (CCMAR-Algarve), University of the Algarve, 8005-139 Faro, Portugal.

Email: eli\_frag@hotmail.com

Ester A. Serrão, Algarve Center of Marine Sciences (CCMAR-Algarve), University of the Algarve, 8005-139 Faro, Portugal.

Email: eserrao@ualg.pt

## Funding information

This study was supported by the Foundation for Science and Technology (FCT) of Portugal through projects UID/Multi/04326/2020 and PTDC/BIA-CBI/6515/2020. J.A. was supported by the transitional norm, DL57/2016/CP1361/CT0035, E.F. by the fellowship SFRH/BD/144878/2019 and E.A.S. by a Pew Marine Fellowship. D.K.-J. was

## Abstract

**Aim:** Marine forests of brown macroalgae create essential habitats for coastal species and support invaluable ecological services. Here, we provide the first global analysis of species richness and endemism of both the kelp and fucoid biomes.

**Location:** Global.

**Time period:** Contemporary.

**Major taxa studied:** Marine forests of brown macroalgae, formed by kelp (here defined as orders Laminariales, Tilipteridales and Desmarestiales) and fucoid (order Fucales), inhabiting subtidal and intertidal environments.

**Methods:** We coupled a large dataset of macroalgal observations (420 species, 1.01 million records) with a high-resolution dataset of relevant environmental predictors (i.e., light, temperature, salinity, nitrate, wave energy and ice coverage) to develop stacked species distribution models (stacked SDMs) and yield estimates of global species richness and endemism.

**Results:** Temperature and light were the main predictors shaping the distribution of subtidal species, whereas wave energy, temperature and salinity were the main predictors of intertidal species. The highest regional species richness for kelp was found in the north-east Pacific (maximum 32 species) and for fucoids in south-east Australia (maximum 53 species), supporting the hypothesis that these regions were the evolutionary sources of global colonization by brown macroalgae. Locations with low species richness coincided between kelp and fucoid, occurring mainly at higher latitudes (e.g., Siberia) and the Baltic Sea, where extensive ice coverage and low-salinity regimes prevail. Regions of high endemism for both groups were identified in the Galapagos Islands, Antarctica, South Africa and East Russia.

**Main conclusions:** We estimated the main environmental drivers and limits shaping the distribution of marine forests of brown macroalgae and mapped biogeographical centres of species richness and endemism, which largely coincided with the expectation from previous evolutionary hypotheses. The mapped biodiversity patterns can serve as new baselines for planning and prioritizing locations for conservation, management and climate change mitigation strategies, flagging threatened marine forest regions under different climate change scenarios.

supported by the Independent Research Fund Denmark (8021-00222 B, "CARMA")

Editor: Derek Tittensor

## KEY WORDS

biodiversity patterns, brown macroalgae, endemism, fucoid, kelp, macroecology, marine forests, species distribution modelling, species richness

## 1 | INTRODUCTION

Global species richness and endemism patterns are the outcome of evolutionary and ecological processes driven by large-scale geological events and long-term climate characteristics and fluctuations (Wiens & Donoghue, 2004). Understanding and estimating these patterns has been a longstanding challenge, yet it remains a fundamental step in ecological, evolutionary and conservation studies (Costello et al., 2017; Tittensor et al., 2010). Importantly, human-induced pressures are changing the distribution of species at global scales (Pecl et al., 2017), a process that has called for the protection of 30% of the oceans by 2030 and that raises the need for a timely estimate of the location of hotspots of species richness and centres of endemism (Zhao et al., 2020).

Species richness and endemism are fundamental metrics of biodiversity and indicators of high conservation value. Nonetheless, current knowledge remains heavily biased toward specific marine taxa (mostly fish, mammals, corals and bivalves) and specific regions, owing to insufficient data (e.g., Selig et al., 2014; Taheri et al., 2021; Tittensor et al., 2010). Although online repositories containing large amounts of data [e.g., Ocean Biogeographic Information System (OBIS) and Global Biodiversity Information Facility (GBIF)] provide new opportunities to broaden our knowledge of distributional patterns for a wider spectrum of marine species (e.g., Chaudhary et al., 2016; Costello et al., 2017; Kusumoto et al., 2020; Selig et al., 2014), they are still incomplete and prone to spatial and taxonomic errors (e.g., Assis et al., 2020). Macroalgae are one such under-represented example in global biodiversity assessments, with many studies concentrated in a few geographical regions.

Macroalgae can form productive marine forests that provide habitat and food to numerous associated species and support key ecosystem services, including food provision and security, shoreline protection from wave energy, nutrient cycling and carbon fixation (e.g., Arafeh-Dalmau et al., 2020; Coleman & Wernberg, 2017; Krause-Jensen et al., 2018; Wernberg et al., 2019). Despite their importance, global biodiversity patterns at the species level are still restricted to taxa of the orders Bryopsidales (green algae) and Dictyotales (brown algae), mainly owing to the lack of reliable data and poor taxonomic resolution (Kerswell, 2006; Verbruggen et al., 2009; Vieira et al., 2021). Additional studies have been conducted at the genus level, which is not necessarily representative of the overall biodiversity (Keith et al., 2014; Kerswell, 2006). Besides, distinct lineages of macroalgae are expected to have distinct richness and endemism patterns, reflecting their evolutionary histories and tendencies to retain or evolve macroecological preferences (Keith et al., 2014; Verbruggen et al., 2009; Vieira et al., 2021).

In the present study, we estimate global patterns of species richness and centres of endemism and explore the underlying macroecological drivers shaping the distribution of brown macroalgal species of kelps (a common name used with a variety of definitions, but here defined as the orders Laminariales, Tilopteridales and Desmarestiales) and fucoids (order Fucales). Below, we use the common designation "marine forests" to refer to the assembly of all these macroalgal orders. To address and overcome the information challenges and gaps previously highlighted, we fitted species distribution models (SDMs; Anderson et al., 2011) and stacked them into layers representing global biodiversity patterns (Guisan & Rahbek, 2011). Stacked species distribution modelling (stacked SDM) is widely used to estimate community composition and generally outperforms other approaches, such as macroecological models, which lack this ability (e.g., Cooper & Soberón, 2018; Mendes et al., 2020). The models used a machine learning algorithm to examine the relationship between biologically relevant predictors (Assis et al., 2017; Fragkoupolou et al., 2021) and quality-controlled occurrence records derived from a recently published large dataset of marine forests (Assis et al., 2020). This approach also allowed us to account for key dispersal and ecological constraints (Mendes et al., 2020). Our results provide global biodiversity maps and environmental limits of regions with distinct levels of species diversity and endemism for 420 species of kelps and fucoids.

## 2 | METHODS

### 2.1 | Occurrence records and environmental data

Occurrence records of kelps (for the purpose of the present framework defined as the orders Laminariales, Tilopteridales and Desmarestiales) and fucoids (order Fucales) were gathered from the curated dataset of 549 species of marine forests (Assis et al., 2020). The dataset comprises multiple sources that were cross-validated against the most recent taxonomic data available in the World Register of Marine Species (WoRMS; Horton et al., 2021) and curated by experts to remove potential geographical errors. The dataset contains observations largely matching the time window of the environmental predictors (c. 80% records after 2000; see next paragraph; Assis et al., 2020). Given that robust species distribution models require a minimum of five geographically distinct occurrence records (van Proosdij et al., 2016), 16 kelp and 113 fucoid species were removed from the dataset. The exclusion of these species did not affect the overall patterns of biodiversity, and no relationship was found between sampling effort and the estimates of species richness (Supporting Information S1). The final dataset contained distribution records for 420 species of brown macroalgae, 96 of the

127 accepted species of Laminariales (76%), 7 of 21 Tilipteridales (33%), 10 of 27 Desmarestiales (37%) and 307 of 564 Fucales species (54%; Guiry & Guiry, 2021).

Biologically relevant predictors for near-present-day conditions were extracted from Bio-ORACLE (long-term average climatologies between 2000 and 2017) for the subtidal (i.e., along the seafloor layers) and intertidal (surface layers) zones, depending on the species distributions (Assis, Tyberghein, et al., 2017; Tyberghein et al., 2012). Light availability, temperature (minimum and maximum), nitrate, salinity, wave energy and sea ice coverage were selected as potential predictors for both subtidal and intertidal species. Low-altitude cloud fraction and maximum air temperature were added for intertidal species (i.e., aerial data). Maximum wave energy was considered for both intertidal and subtidal macroalgae, in order to account for high-energy environments. This layer was produced to match the Bio-ORACLE 5 arcmin resolution with the nearest neighbour algorithm based on the classification developed by Fairley et al. (2020). This used the ECMWF ERA5 reanalysis to provide six classes of wave energy at 0.5° resolution, with one representing enclosed seas with calm conditions and six the highest-energy oceanic coasts, influenced by large, long-period swells and storm conditions (Fairley et al., 2020). Before modelling, collinearity between predictors was assessed with Pearson's correlation coefficient and the variance inflation factor (VIF; Araújo et al., 2019; Harisena et al., 2021). If a high correlation was found between predictor pairs ( $>0.8$ ; Assis, Araújo, et al., 2017), only one was included in the models.

## 2.2 | Stacked species distribution modelling

Individual SDMs were produced with BOOSTED REGRESSION TREES (BRT; De'ath, 2007), a machine learning algorithm that combines the advantages of regression trees and boosting, able to fit nonlinear relationships between response (occurrence data) and predictor variables (environmental data), with demonstrated high predictive performance (Assis, Araújo, et al., 2017; Elith et al., 2006; Fragkopoulou et al., 2021). Moreover, proper hyperparametrization (see next paragraph) and the ability to force monotonicity responses strongly reduces overfitting of BRT and therefore increases the potential for model transferability (Elith et al., 2008; Hofner et al., 2011).

Given that BRT requires both presence and absence data and that only presences were available, a minimum number of 1,000 pseudo-absences or the same number as presences (if  $>1,000$ ) were randomly generated in sites where no presences were recorded for the species being modelled (Barbet-Massin et al., 2012). This process was geographically limited to the ecological provinces (Spalding et al., 2007) where the species occurs, in addition to their neighbouring ecological provinces (Araújo et al., 2019), to limit pseudo-absences to regions where species were not recorded but where dispersal might occur, which is a crucial step in SDM development (Assis, Araújo, et al., 2017; Barve et al., 2011).

To reduce surplus information and the negative effect of autocorrelation in the models (Dormann et al., 2007), the correlation of

predictors within the range of occurrence records (presence and pseudo-absences) was tested as a function of geographical distance. For this purpose, correlograms were built to pinpoint the minimum geographical distance at which predictors were significantly correlated. Records per species were pruned by randomly selecting one record from the pool found within such distances (e.g., Assis, Araújo, et al., 2017; Fragkopoulou et al., 2021).

Models fitted records per species (presences and pseudo-absences) against predictor variables using the GBM package, and hyperparametrization was optimized through cross-validation by partitioning data into six independent latitudinal bands. In this process, models were trained interactively with all hyperparameter combinations (i.e., the "grid search" method) of the number of trees (from 50 to 1,000, in steps of 50), learning rate (0.01 and 0.001) and tree complexity (from one to six, in steps of one). Predictive performance of the models was evaluated in one latitudinal band withheld at a time with the area under the curve (AUC) of the receiver operating characteristic curve (Fielding & Bell, 1997). The optimal hyperparameter combination that reduced overfitting and increased transferability was found as the one producing models with higher AUC in cross-validation (Assis, Araújo, et al., 2017; Vignali et al., 2020). The cross-validation framework also allowed inference of the final performance of the models tuned with the optimal hyperparameters in independent data (Assis, Araújo, et al., 2017; Fragkopoulou et al., 2021; Vignali et al., 2020). Overfitting was controlled further through the forcing of specific monotonic responses to the predictors (i.e., negative or positive influence; Hofner et al., 2011). Specifically, negative responses were set for maximum temperature, ice coverage and maximum wave energy, because higher values along environmental gradients can explain the absence of macroalgae (Assis, Araújo, et al., 2017; Cavanaugh et al., 2011), and positive responses for the remaining predictors, because lower values can explain absences (Assis, Araújo, et al., 2017; Fragkopoulou et al., 2021; Gouvêa et al., 2020). Assigning a monotonic response does not predefine the range of values setting the response of models (presence or absence), but rather the trend of model fitting based on ecological theory (Hofner et al., 2011).

The relative contribution of predictors to the models was determined by computing the increase in AUC when each predictor was added to its alternative model (i.e., the one including all predictors except that being tested). Physiological tolerance limits (maximum and minimum, depending on the predictor) were estimated from individual response functions produced for each predictor, while fixing all alternative predictors to their averages (Assis, Araújo, et al., 2017; Elith et al., 2008). Final models were built by discarding predictors with residual or negative contributions through a stepwise approach based on AUC. To this end, a full model was fitted (i.e., with all predictors) and predictors were removed interactively one at the time, from the least to the highest contributive until the difference of AUC between the full model and the reduced model was higher than zero (Elith et al., 2008; Fragkopoulou et al., 2021). This resulted in parsimonious models (i.e., with fewer predictors), which tend to be more robust to the effects of multicollinearity in

the data (Dormann et al., 2013) and have occasionally been shown to have higher spatial and temporal transferability (Randin et al., 2006; Sequeira et al., 2018; but for a more thorough evaluation of the trade-offs between model complexity and predictive power, see García-Callejas & Araújo, 2016).

Maps reflecting the potential distribution of each species (i.e., habitat suitability) were developed for global shorelines with the selected parsimonious models. These maps were reclassified into binomial surfaces reflecting presence and absences by applying a threshold maximizing both specificity (true-negative rate) and sensitivity (Fielding & Bell, 1997). To account for dispersal constraints, maps per species were clipped to suitable reachable areas, an approach that reduces potential overprediction, with no increase in underprediction (Mendes et al., 2020; Thuiller et al., 2004). Suitable reachable areas were defined as those with continuous habitat suitability, where at least one occurrence was recorded. This assumes that a species cannot cross a potential dispersal barrier defined by unsuitable conditions, unless demonstrated by occurrence records (Ballesteros-Mejia et al., 2017; Cooper & Soberón, 2018). This was implemented by eliminating predicted areas of habitat suitability where no occurrence records existed. Final predictive performance was assessed with AUC and true skill statistic (TSS; Allouche et al., 2006) for both maps, clipped and unclipped to reachable areas.

The contributions of predictors and physiological thresholds defining distributions were calculated as the average of individual SDMs for kelps and fucoids. Potential species richness was inferred for the two groups by stacking predictions from individual SDMs with a sum function (i.e., binary stacked SDMs; Guisan & Rahbek, 2011). Given that estimates of species richness are scale dependent (Kusumoto et al., 2020), we inferred the optimal resolution of the standardized Uber's hexagonal hierarchical spatial data (Bondaruk et al., 2020) by computing the average difference between observed and predicted species richness when aggregated at each resolution of hexagon shapes. Uber's hexagonal framework was chosen owing to its equal-area projection and optimal indexing algorithm, which allows fast data aggregation over its hierarchical resolutions (Bondaruk et al., 2020).

Furthermore, the local (i.e., per hexagon) species range rarity was quantified as a measure of endemism by the corrected endemism index (CWEI; Crisp et al., 2001; Schmitt et al., 2017). The weighted endemism index (WEI; Equation 1) for the hexagon  $c$  ( $WEI_c$ ) was calculated by summing the inverse of the geographical range size  $r_{i,c}$  for each of the  $n_c$  species. In this way, species with a smaller geographical range were assigned a larger weight. To reduce correlation between species richness and endemism, the corrected endemism index for the hexagon  $c$  ( $CWEI_c$ ; Equation 2) was calculated as the weighted endemism index  $WEI_c$  divided by the total number of species  $RS_c$  found within each hexagon  $c$  (Crisp et al., 2001; Schmitt et al., 2017).

$$WEI_c = \sum_{i=1}^{n_c} \left( \frac{1}{r_{i,c}} \right) \quad (1)$$

$$CWEI_c = \frac{WEI_c}{RS_c} \quad (2)$$

All analyses were performed using R (R Development Core Team, 2021).

### 3 | RESULTS

The final occurrence dataset to produce individual SDMs comprised 113 kelp (628,425 occurrence records) and 307 fucoid species (383,958 records), of which 36 were intertidal (Supporting Information S2). Overall, models achieved high performance in predicting species occurrence for both kelps (cross-validation AUC:  $.87 \pm .07$ ; AUC:  $.98 \pm .02$ ; TSS:  $.92 \pm .07$ ) and fucoids (cross-validation AUC:  $.95 \pm .08$ ; AUC:  $.98 \pm .01$ ; TSS:  $.93 \pm .07$ ; Supporting Information S3). The performance of the models improved significantly when accounting for dispersal constraints across unsuitable habitats (i.e., clipping to suitable reachable areas; significant increases for kelp:  $\Delta$ AUC:  $.02 \pm .01$ ,  $\Delta$ TSS:  $.06 \pm .02$ ; and fucoids:  $\Delta$ AUC:  $.02 \pm .01$ ,  $\Delta$ TSS:  $.06 \pm .03$ ; Wilcoxon signed-rank test).

The distribution of subtidal kelp and fucoid species was best explained by light and temperature (minimum and maximum; relative contributions averaged for kelps and fucoids  $>10\%$ ; Table 1). Intertidal distributions were best explained by wave energy, temperature (minimum and maximum) and salinity (relative average contributions  $>10\%$ ; Table 1). Nitrate concentration and sea ice coverage had a lower contribution to the models (c. 5%–10%; Table 1), yet the distribution limits of some species were strongly shaped by thresholds defined by these predictors (95th percentile of contributions 19%–38% for both subtidal and intertidal species; Table 1). Cloud fraction and maximum air temperature made small contributions to the models for intertidal species (contributions c. 5%; Table 1; Supporting Information S4). These findings are reinforced by the overall low collinearity between predictors (Supporting Information S5); only minimum and maximum sea temperatures showed stronger collinearity for subtidal species, and maximum air and sea temperatures for intertidal species (Pearson's correlation  $>.85$ ; VIF  $> 5$ ; Supporting Information S5). However, their opposite monotonic fit in BRT (negative for maximum temperatures and positive for minimum temperatures) allowed removal of confounding inferences about the contribution of predictors.

Physiological thresholds, averaged from independent partial dependency plots developed per species (Table 1), showed favourable habitat conditions for the whole kelp biome for temperatures between 2.7 and 23.7°C (95th percentile  $-1.8$  and  $32.5^\circ\text{C}$ ; long-term average of minimum and maximum temperatures across species) and light  $>0.24 \text{ E}/\text{m}^2/\text{year}$ . Favourable conditions for subtidal fucoids were estimated to temperatures between 9.4 and 28.7°C (95th percentile  $-1.8$  and  $34.9^\circ\text{C}$ ) and light  $>1.11 \text{ E}/\text{m}^2/\text{year}$ . Intertidal fucoids showed lower thermal tolerances within 2.5 and 22.8°C (95th percentile between  $-1.8$  and  $28.6^\circ\text{C}$ ), a maximum wave energy of class 5 (95th percentile between 1 and 6) and salinity  $>16$  (95th percentile between 3.3 and 34.6; Supporting Information S4).

Stacking individual SDMs allowed estimation of the distribution of species richness patterns. These patterns were best estimated

TABLE 1 Average relative contribution (as a percentage) of each environmental predictor to the performance of models (bold depicting average contributions >10%) and thresholds reflecting physiological tolerance limits for marine forests of kelp, intertidal fucoid and subtidal fucoid

Predictors	Kelp			Subtidal fucoid			Intertidal fucoid		
	Contribution	Threshold	Contribution	Threshold	Contribution	Threshold	Contribution	Threshold	Contribution
Light (E/m <sup>2</sup> /year)	<b>39 (7-74)</b>	0.24 (0-0.8)	<b>36 (1-71)</b>	1.11 (0-6.32)	–	–	–	–	–
Minimum temperature (°C)	<b>27 (0-54)</b>	2.7 (-2.1-14.6)	<b>20 (0-51)</b>	9.4 (-1.9-21.8)	<b>28 (0-97)</b>	2.5 (-1.8-11)	2.5 (-1.8-11)	2.5 (-1.8-11)	2.5 (-1.8-11)
Maximum temperature (°C)	<b>16 (0-40)</b>	23.7 [14.1-32.6]	<b>21 (0-47)</b>	28.7 (21-35)	<b>11 (0-50)</b>	22.8 [16.9-28.6]	22.8 [16.9-28.6]	22.8 [16.9-28.6]	22.8 [16.9-28.6]
Wave exposure (class)	<b>9 (0-40)</b>	5 (4-6)	<b>12 (0-42)</b>	5 (1-6)	<b>28 (0-93)</b>	5 (1-6)	5 (1-6)	5 (1-6)	5 (1-6)
Salinity (PSS)	<b>2 (0-9)</b>	15 (0-33)	<b>4 (0-36)</b>	18 (0-35)	<b>12 (0-62)</b>	16 (3-35)	16 (3-35)	16 (3-35)	16 (3-35)
Nitrate (mmol/m <sup>3</sup> )	<b>6 (0-24)</b>	0.88 (0-5.7)	<b>8 (0-32)</b>	0.24 (0-0.6)	<b>6 (0-23)</b>	0.43 (0-3.2)	0.43 (0-3.2)	0.43 (0-3.2)	0.43 (0-3.2)
Sea ice thickness (m)	<b>2 (0-19)</b>	0.2 (0-0.9)	<b>5 (0-34)</b>	0.14 (0-0.7)	<b>9 (0-38)</b>	0.1 (0-0.3)	0.1 (0-0.3)	0.1 (0-0.3)	0.1 (0-0.3)
Cloud fraction (0-1)	–	–	–	–	–	–	–	–	–
Maximum air temperature (°C)	–	–	–	–	–	–	–	–	–

Note: Parentheses indicate the 5th and 95th percentiles of values.

with a 60 km edge length resolution (hexagon area: 9,353 km<sup>2</sup>) of Uber's global grid system (Figure 1). At this resolution, the average difference between observed and predicted species richness was 0.96 (i.e., 0.96 more species predicted than observed), with a Pearson correlation of .85 (Figure 1).

Overall, the suitable geographical area estimated for kelp (1,705,227 km<sup>2</sup>) was smaller than for fucoids (2,574,986 km<sup>2</sup>), but the two groups had some overlap in suitable regions (Supporting Information S6). Species richness patterns differed latitudinally, with peaks of diversity in distinct regions for kelps and fucoids and overall endemicity regions coinciding, although with some differences between the two groups (Figures 2 and 3). Kelps exhibited a latitudinal bimodal species richness distribution, with a minimum near the equator and peaks between 13 and 77 °N and between 5 and 64 °S (Figure 2a). The highest species richness was found in the north-east Pacific (32 species), with numerous regional hotspots from Alaska to Baja California. Additional hotspots were estimated in the Atlantic regions of Greenland to Newfoundland (Canada), and along the Atlantic coast of Europe; in the west Pacific, hotspots were estimated from the Okhotsk Sea to South Korea. In the Southern Hemisphere, species richness was lower (maximum 10 species), with the richest regions along the shorelines of south-east Australia and New Zealand. Low kelp species richness (i.e., poor-spots) were predicted at higher latitudes, but extended along large areas (e.g., *Alaria marginata* and *Laminaria solidungula*), such as in North and South America and North Russia, associated with ice-driven or river-discharge salinity minima. Poor-spots were also predicted in the warm regions of the Mediterranean, the Red Sea and South China (Figure 2a). Highest kelp endemicity was predicted in the Galapagos Islands (*Eisenia galapagensis*), Chile (*Lessonia spicata* and *Lessonia berteroana*), Brazil (*Laminaria abyssalis*), the Falkland Islands (*Lessonia searlesiana*), Antarctica (*Desmarestia confervoides*, *Desmarestia menziesii* and *Desmarestia chordalis*), South Africa (*Ecklonia maxima* and *Laminaria pallida*), Heard Island and McDonald Islands (Southern Ocean islands) and East Russia (Sakhalin and Kuril Islands; *Saccharina gyrata*; *Saccharina cichorioides f. coriacea*; Figure 2b; Supporting Information S7).

Furoid species were distributed from 171 °N to 64 °S (Figure 3a). Highest richness was predicted in South Australia (53 species), with numerous hotspots from Brisbane to Kalbarri. Additional hotspots were predicted in New Zealand, in the Indo-Pacific (Indonesia), north-west Pacific along the coasts of Japan and Guangdong, China, North Atlantic from Norway to Morocco, around Iceland and along the Newfoundland coast (Figure 3a). Poor-spots were mostly predicted in the south-east Pacific (Chile), the south-east Mediterranean and the Black Sea. Furoid endemicity was predicted in Hawaii, Baja California (*Stephanocystis setchellii*, *Stephanocystis dioica*, *Sargassum johnstonii* and *Sargassum sinicola*), the Galapagos Islands and continental Ecuador (*Sargassum galapagense*, *Sargassum ecuadoreanum* and *Sargassum setifolium*), Antarctica (*Cystosphaera jacquinotii*), South Africa (*Bifurcariopsis capensis*, *Brassicophycus sisymbrioides* and *Cystophora fibrosa*), the Red Sea and the Arabian Peninsula

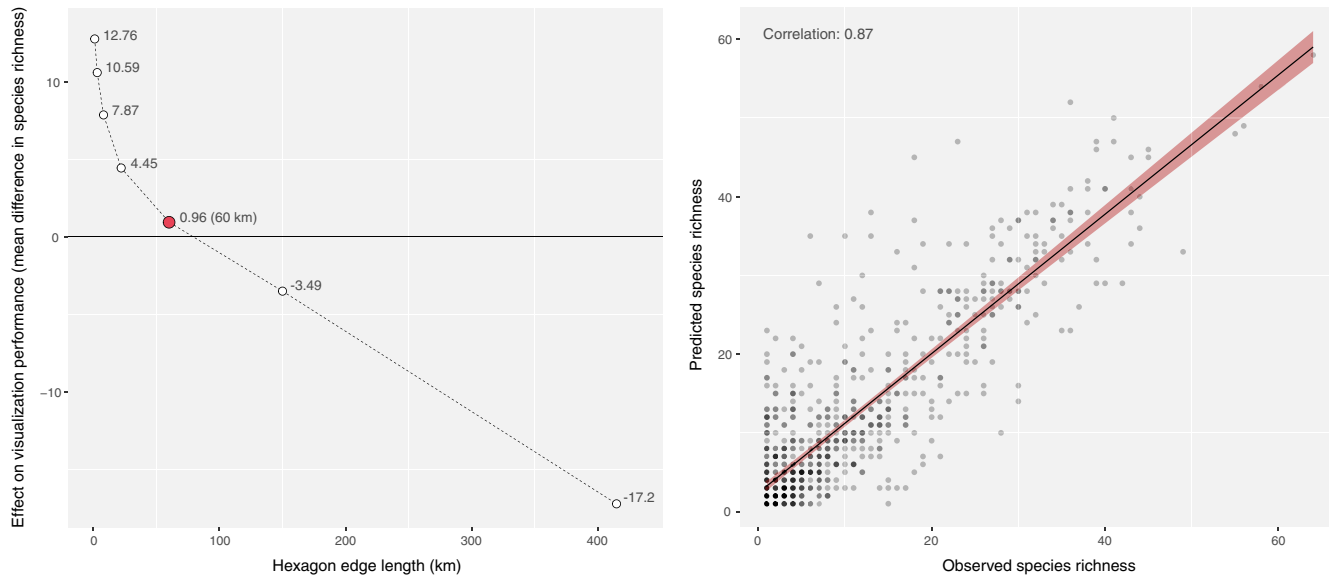


**FIGURE 1** (a) Difference between observed and predicted species richness in relationship to the resolution of hexagon shapes. (b) Correlation between observed and predicted potential species richness at the optimal resolution of hexagon shapes (60 km)

(*Sargassum dentifolium*, *Sargassum boveanum* and *Sargassum acinaciforme*), South China (*Sargassum herklotsii* and *Sargassum quinhonense*), Japan and East Russia (Sakhalin and Kuril Islands; *Sargassum yendoi*, *Sargassum ammophilum* and *Coccophora langsdorffii*), south-east Australia (*Cystophora xiphocarpa* and *Carpoglossum confluens*) and New Zealand (*Durvillaea willana*; Figure 3b; Supporting Information S8).

Predictive layers per species are available in Supporting Information S9.

## 4 | DISCUSSION

Using stacked SDMs, we estimated the global distribution of species richness and endemism of kelps and fucoids; a goal hindered previously by insufficient or unreliable data. The geographical centres of species richness identified were strongly driven by thermal affinities. Centres of higher species richness were found in the north-east Pacific ( $\leq 32$  species of kelps) and south-east Australia ( $\leq 53$  species of fucoids). These hotspots differ from those identified previously for the predominantly tropical macroalgal orders Bryopsidales (Indo-Australian Archipelago; Kerswell, 2006) and Dictyotales (Central Indo-Pacific; Vieira et al., 2021) and also between intertidal and subtidal species, consistent with the geography of their evolutionary origin. In contrast, poor-spots of species richness coincided between kelps and fucoids (e.g., higher latitudes; Figures 2a and 3a), in line with previous studies (Kerswell, 2006; Vieira et al., 2021). In the same way, regions with high endemism coincided for kelps and fucoids, mainly identified in climatically stable and isolated regions of the Galapagos Islands, Antarctica, South Africa, Japan and East Russia (Sakhalin and Kuril Islands; Figures 2b and 3b; Harrison & Noss, 2017).

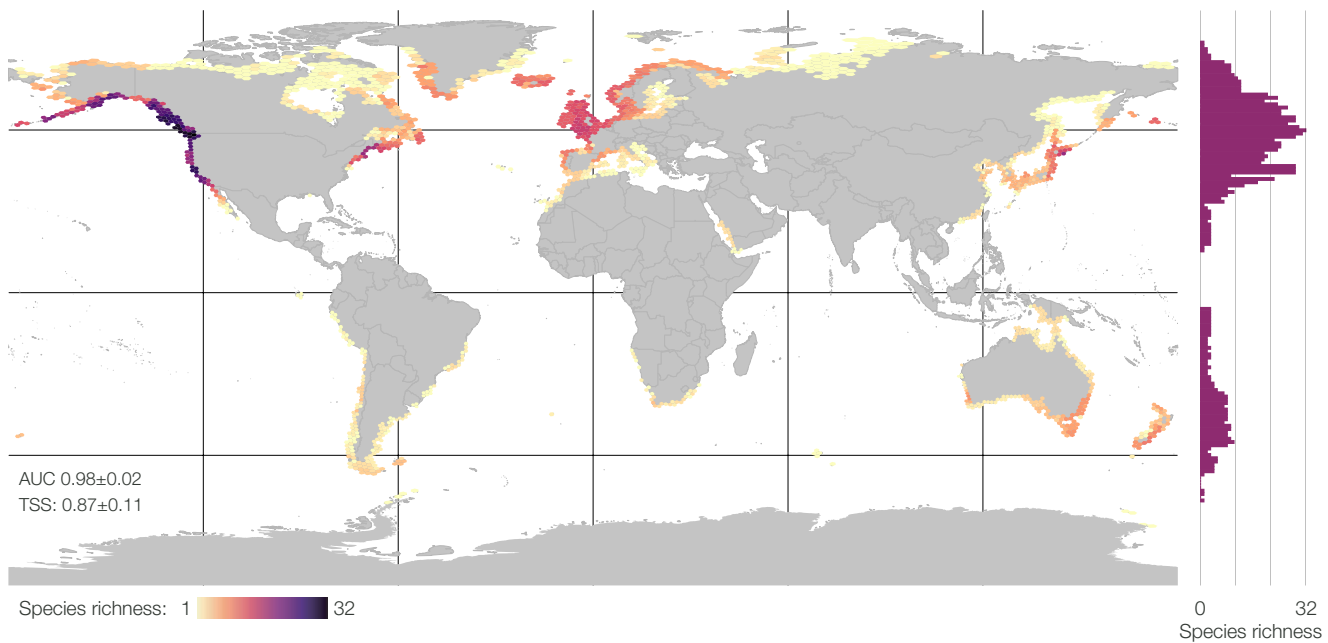
### 4.1 | Performance of stacked SDMs

The selection of relevant predictors, taking into consideration important physiological drivers (e.g., light availability for photosynthesis), resulted in models with high performance (average AUC  $> .98$  and TSS  $> .92$ ). When combined with dispersal constraints, performance was improved further ( $\Delta$ AUC: .02;  $\Delta$ TSS: .06) by reduction of overprediction, a common but often neglected SDM approach (Mendes et al., 2020) that does not require the consideration of information on species-specific dispersal ecology (Cooper & Soberón, 2018), which is largely unavailable (Assis et al., 2021). Estimates of species richness were produced globally at the scale of 60 km, overestimating by only approximately one species, when compared to the real observed data. This might indicate that the potential niche is often realized at these scales, where community interactions, such as grazing and competition, in addition to temporal fluctuations in occurrence, do not affect the regional distribution.

### 4.2 | Environmental niches

The results showed that temperature, light and wave energy are key predictors of the environmental niche of 420 kelp and fucoid species. This is in line with previous studies at macroecological scales that have shown light and temperature regimes to be drivers for the distribution of marine biodiversity (Gagné et al., 2020). For macroalgae, besides temperature and light, wave energy, nutrients and salinity have also been identified as additional macroecological drivers (Cavanaugh et al., 2011; Jayathilake & Costello, 2020, 2021; Keith et al., 2014; Wernberg et al., 2019; Wilson et al., 2019). Overall, favourable conditions for subtidal

(a) Laminariales, Tilipteridales &amp; Desmarestiales



(b)

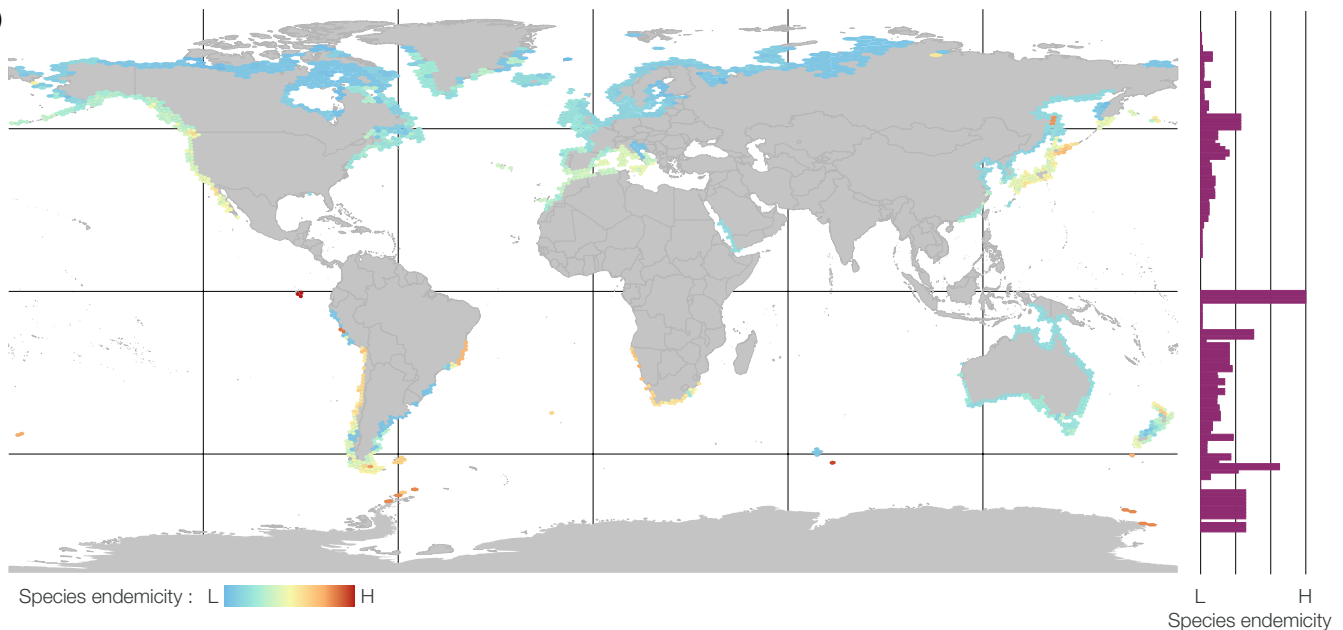
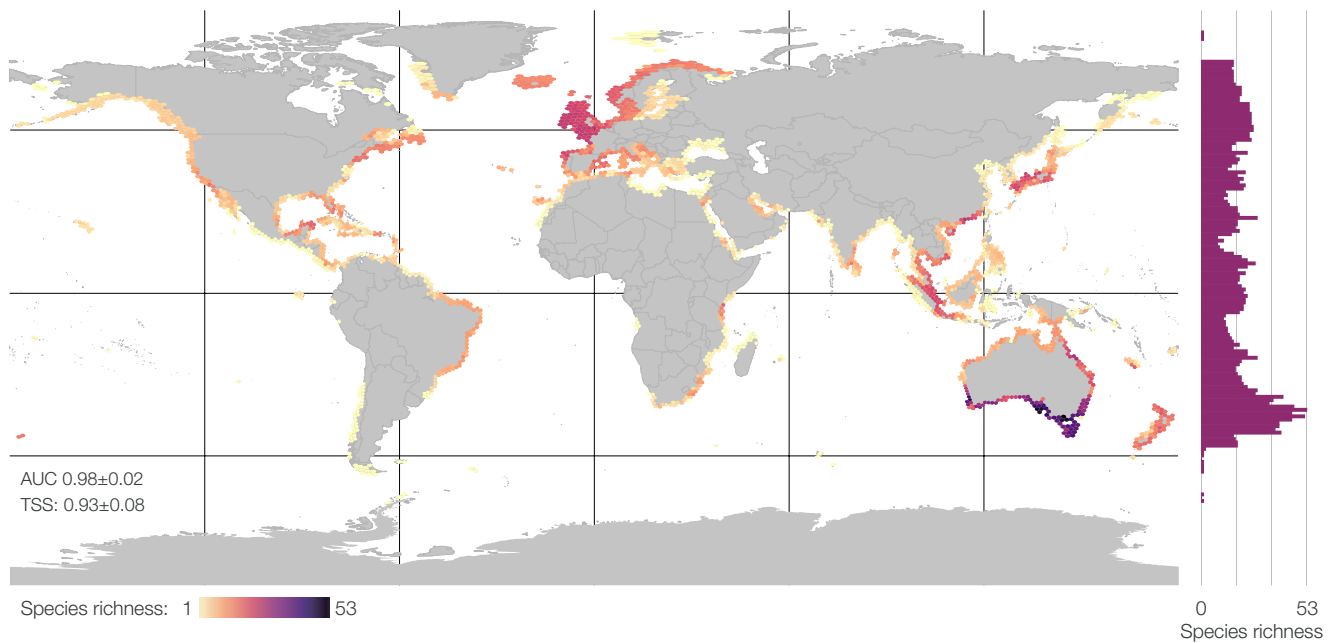


**FIGURE 2** Global estimates of kelp (a) species richness and (b) endemicity for an optimal resolution of the global hexagon grid system (60 km). Species richness and endemicity by latitudinal bins of 0.5° resolution are presented in the side graphs. Estimates of endemicity have been  $\log_{10}$  transformed to enable the visualization of the zero-skewed values of low (L) and high (H) levels of endemicity

species were shaped primarily by light availability (kelps:  $>0.24 \text{ E/m}^2/\text{year}$ ; fucoids:  $>1.11 \text{ E/m}^2/\text{year}$ ) and temperature at the seafloor (kelps: 2.8–23.7°C; fucoids: 9.4–28.7°C); whereas favourable conditions for intertidal fucoids were shaped by high wave energy (class 5; Fairley et al., 2020), sea surface temperatures (2.5–22.8°C) and salinity ( $>16.02 \text{ PSS}$ ). Environmental drivers such as ice cover contributed less on average to the models, but had high contribution to species that reach higher latitudes (Table 1; Supporting Information S4), owing to the ice scouring effect for intertidal organisms and attenuation of light availability for subtidal

organisms (Assis, Araújo, et al., 2017; Krause-Jensen et al., 2012). Likewise, salinity made an increased contribution to species distributed along the Baltic Sea (Schubert et al., 2011), the Hudson Bay (Assis et al., 2014) and the Siberian shelf, where the world's largest rivers discharge. Together, these drivers shaped kelp and fucoid biomes, matching well-described biogeographical limits, such as those in Baja California (Cavanaugh et al., 2019), Morocco (Assis et al., 2014; Lourenço et al., 2016), South Africa (Anderson et al., 2007) and Kalbarri (Australia; Wernberg et al., 2013), in addition to regions with extremely cold environments, low-salinity

(a) Fucales



(b)

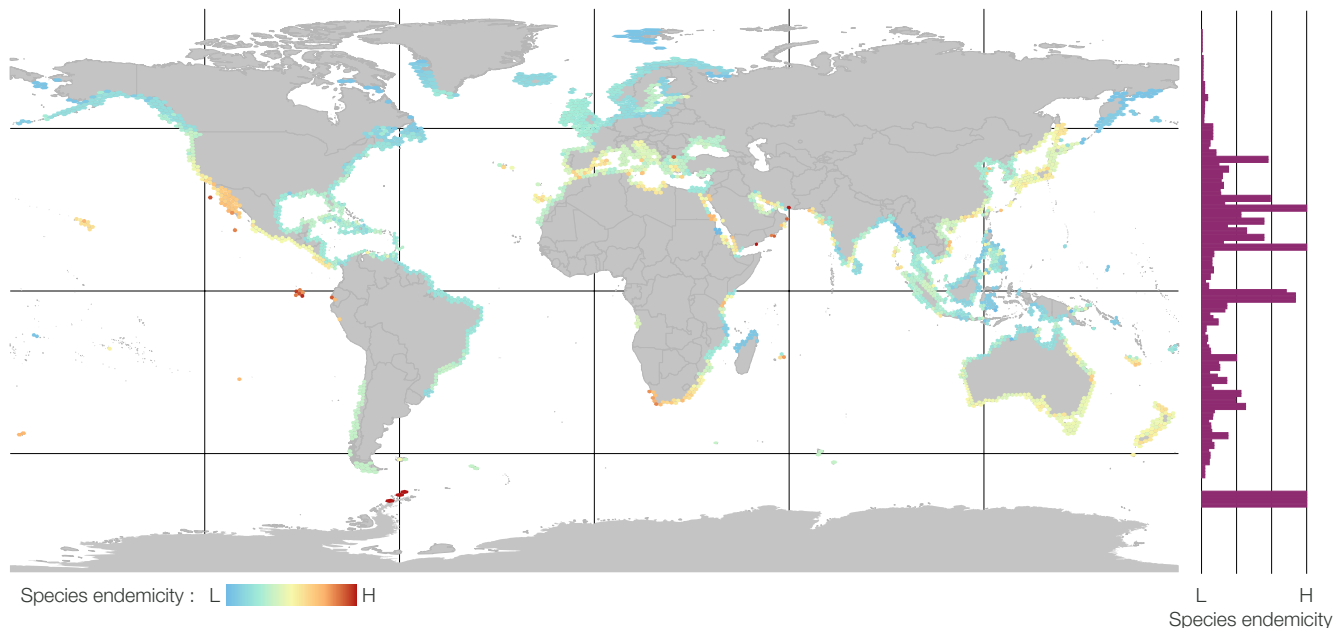


**FIGURE 3** Global estimates of fucoid (a) species richness and (b) endemicity for an optimal resolution of the global hexagon grid system (60 km). Species richness and endemicity by latitudinal bins of 0.5° resolution are presented in the side graphs. Estimates of endemicity have been  $\log_{10}$  transformed to enable the visualization of the zero-skewed values of low (L) and high (H) levels of endemicity

regimes and extensive ice coverage (Jayathilake & Costello, 2020; Kerswell, 2006; Vieira et al., 2021).

#### 4.3 | Predicted suitable areas

Although higher resolution is preferred to detect patchy patterns in the distribution of kelps and fucoids accurately, suitable areas for kelps were predicted to cover c. 1.71 million km<sup>2</sup>, matching the scale

of previous studies (2 million km<sup>2</sup>; Jayathilake & Costello, 2021). Fucoids had a larger predicted suitable habitat area than kelps, covering c. 2.57 million km<sup>2</sup>, a first global estimate for this group. This might place fucoids as the largest marine biome mapped to date, greater in relative area than the kelp, but also seagrass, mangrove and zooxanthellate coral biomes (Jayathilake & Costello, 2021). Furthermore, our study did not consider the pelagic fucoid species of the genus *Sargassum*, which might occupy an additional area (Gouvêa et al., 2020).

#### 4.4 | Kelp diversity

The inferred patterns of species richness (poor-spots and hotspots) and endemicity of brown macroalgae were considered in light of existing biogeographical and evolutionary hypotheses (Costello et al., 2017; Harrison & Noss, 2017; Verbruggen et al., 2009). Specifically for kelp, the highest regional species richness found along the coasts of California and Alaska, followed by hotspots in the Okhotsk and Japan–Korea regions, the North Atlantic and the Arctic (Figure 2a), match phylogenetic hypotheses raised by previous studies. These suggest that kelp originated in the north-east Pacific (where higher richness was predicted), later colonized the north-west Pacific and, after recurrent trans-Arctic passages, invaded and colonized the Arctic and North Atlantic Ocean through the opening of the Bering Sea 5.5 Ma (Bolton, 2010; Starko et al., 2019). The high richness estimated for the north-east Atlantic (Figure 2a) could also be explained by the larger number of Quaternary climatic refugia, in comparison to the north-west Atlantic and the Arctic regions, where more extensive coastal ice coverage might have affected populations to a higher degree (Assis, Araújo, et al., 2017; Assis et al., 2014), although this does not preclude Arctic refugia for some species (Bringloe, Verbruggen, et al., 2020).

The general lower species richness (Figure 2a) in the Southern Hemisphere is in agreement with previous colonization hypotheses. For Laminariales, southern colonizations occurred for only the genera *Ecklonia*–*Eisenia* and *Laminaria*, and only the genus *Lessonia* is endemic to the Southern Hemisphere (Supporting Information S6; Bolton, 2010). Antarctica, in particular, is poor in Laminariales kelp species, but rich in endemic species of the genus *Desmarestia*, namely *Desmarestia confervoides*, *Desmarestia menziesii* and *Desmarestia chordalis* (Figure 2b; Supporting Information S7; Bringloe, Starko, et al., 2020), matching the hypothesis of a Southern Hemisphere origin of this family (Peters et al., 1997). Antarctica thus appears to have been kept relatively isolated, probably owing to permanent coastal sea ice cover and seasonal sea ice expansion, in addition to the plausible dispersal barrier represented by the Antarctic Circumpolar Current. This is supported by Antarctica having the highest marine species endemicity (relative to all species) of any continent (Costello et al., 2010, 2017). Besides *Desmarestia* species in Antarctica, kelp endemism is found in long-term stable climatic regions (Harrison & Noss, 2017), including New Zealand and Southern Ocean islands, and poor-spots of South America (e.g., *Laminaria abyssalis* in Brazil; *Eisenia galapagensis* in the Galapagos Islands) and South Africa (*Ecklonia maxima* and *Laminaria pallida*). The main kelp endemism region for the Northern Hemisphere is Eastern Russia (*Saccharina gyrata* and *Saccharina cichorioides f. coriacea*; Figure 2b; Supporting Information S7).

#### 4.5 | Fucoid diversity

The patterns of richness and endemicity of fucoids differed strongly from kelp and matched well the expectation from the evolutionary

hypotheses of the many species that make up the order Fucales, with highest regional species richness in south-east Australia, followed by Indonesia and the north-east Atlantic (Figure 3; Supporting Information S6). These findings are in agreement with hypotheses raised for the family Sargassaceae, which contains >90% of the Fucales species and dominates the patterns of this group (Supporting Information S6; Bringloe, Starko, et al., 2020). The high richness in the tropics and especially in the Indo-Pacific (211 species; Supporting Information S6) reflects the cosmopolitan distribution of the species-rich genus *Sargassum* (Bringloe, Starko, et al., 2020; Yip et al., 2020). *Sargassum* has evolved and radiated massively in the island-rich central Indo-Pacific region, matching our richness patterns, and from there, it diversified across the globe (Yip et al., 2020). The additional rich fucoid families are the Southern Hemisphere Seirococcaceae and the anti-tropical Fucaceae. The latter are hypothesized to have also evolved in Australia–New Zealand (Cánovas et al., 2011; Serrão et al., 1999), dispersed to the northern Pacific and, when the Bering Sea opened 3–5.5 Ma, colonized the Atlantic, where they diversified into multiple lineages (Cánovas et al., 2011; Coyer et al., 2006; Serrão et al., 1999). The high species richness predicted by our models in the North Atlantic (25 vs. 10 Fucaceae species in the North Pacific; Supporting Information S6) agrees with hypotheses of higher speciation owing to multiple independent crossings of the Bering Strait (Cánovas et al., 2011). Regions of higher fucoid endemicity include the poor-spots of the Galapagos Islands, Antarctica and the Arabian Peninsula, and the hotspots of Baja California, South Africa, Japan, South Australia and New Zealand (Figure 3b; Supporting Information S8).

#### 4.6 | Limitations

The models showed high predictive performances but still contain inherent limitations, such as potential data gaps and uneven sampling effort at global scales. Although no spatial relationships were found between sampling effort and species richness (Supporting information S1), spatial biases can impact biodiversity estimates, particularly in undersampled regions, such as the Southern Hemisphere, the tropics and Africa (Taheri et al., 2021). Furthermore, missing information on biotic interactions and abiotic characteristics, such as the type of substratum, could improve the models and coverage estimates, but no such data are currently available at global scales (Jayathilake & Costello, 2020; Kusumoto et al., 2020). Hence, the estimates of area are likely to be overestimates because of the assumption that all substrata are suitable for brown macroalgae, although these are largely restricted to rocky shores or hard substrata. Additionally, the inferred endemism patterns could be conservative or new regions of endemicity could emerge, considering that 16 kelp and 113 fucoid species were removed from the analyses owing to insufficient data for SDMs (Supporting information S1). Nonetheless, the exclusion of these species did not alter the broad patterns inferred (Supporting Information S1), which largely match the existing origin and evolutionary theories of each studied group. Regardless

of the abovementioned handicaps, we were able to produce biodiversity estimates for hundreds of species, an approach never taken before for the ecological groups considered.

## 4.7 | Applications

Our results establish new global baseline information on kelp and fucoid biodiversity that can be used for planning and prioritizing locations for conservation, management and climate change mitigation strategies (e.g., Zhao et al., 2020). Conservation priority efforts could be directed both at species richness and endemicity hot-spots, aiming to protect as much biodiversity as possible (Trebilco et al., 2011; Zhao et al., 2020), and at poor-spots, where habitat provision might depend solely on a few species (e.g., the Galapagos Islands, Antarctica and South Africa; Coleman & Wernberg, 2017; Zhao et al., 2020).

Climate change has been driving the redistribution of marine biodiversity at the global scale (Chaudhary et al., 2021). Marine forests of kelps and fucoids have shifted ranges by hundreds of kilometres on the south-western coast of Australia (Coleman & Wernberg, 2017; Gurgel et al., 2020; Wernberg et al., 2013), California (Cavanaugh et al., 2019), north-west Africa and the Iberian Peninsula (Assis, Berecibar, et al., 2017; Lourenço et al., 2016; Nicastro et al., 2013). In the near future, the physiological limits of macroalgae can be exceeded further in terms of temperature (e.g., heatwaves), light availability (e.g., terrestrial runoff increasing water turbulence), wave energy (e.g., storms) and salinity (e.g., rainfall and ice melting), causing additional losses of local populations (Arafeh-Dalmau et al., 2020). This can be particularly aggravated in regions undergoing rapid climate change, such as the higher latitudes, cold-temperate transitioning zones, the Mediterranean Sea or the tropics (IPCC, 2021).

Future losses could result in ecosystem changes that can affect fisheries and other coastal economic activities (Arafeh-Dalmau et al., 2020; Buschmann et al., 2017). For instance, potential declines of kelp in northern China, Japan and Eastern Russia, where rapid climate changes are anticipated for the future (IPCC, 2021), could impact the global production of macroalgae, considering that China alone is the largest global producer (Buschmann et al., 2017). Combining our estimates with future climate change projections under different mitigation scenarios could flag threatened marine forest regions and highlight the benefits of timely conservation and mitigation actions (Martins et al., 2021).

## 4.8 | Conclusions

We have provided the first global map of biodiversity estimates for kelps and fucoids that can be used for prioritizing areas for management and conservation. The biogeographical centres of species richness were in the north-east Pacific for kelps and in South Australia for fucoids, corroborating the regions of evolutionary origin. Centres

of high endemicity were common between groups, located in climatically stable and isolated regions. At local scales, ecological interactions, such as grazing, affect kelp and fucoid abundance, whereas we found that environmental factors explained their distribution at the spatial scale of our analyses. We estimate the environmental limits of the kelp biome to be within thermal conditions of 2.7–23.7°C and light >0.24 E/m<sup>2</sup>/year, and for the fucoid biome to be within 2.5–28.7°C and light >1.11 E/m<sup>2</sup>/year. Thus, if environmental conditions alter owing to future climate change, marine forest ranges and therefore biodiversity patterns could shift, particularly where species are at the edge of their physiological limits.

## CONFLICT OF INTEREST

The authors declare no conflict of interest.

## DATA AVAILABILITY STATEMENT

The authors declare that all occurrence records were gathered from the fine-tuned dataset of marine forest species (Assis et al., 2020). Environmental predictors were downloaded from Bio-ORACLE (Assis, Tyberghein, et al., 2017). The wave energy predictor was developed by Fairley et al. (2020). Additional information on predictive performance of models, species richness estimates and the predictive layers per species and stacked species distribution estimates are openly available as supporting information in Figshare at: <https://doi.org/10.6084/m9.figshare.14496018.v4>

## ORCID

Eliza Fragkopoulou  <https://orcid.org/0000-0002-0557-3954>  
 Carlos M. Duarte  <https://orcid.org/0000-0002-1213-1361>  
 Jorge Assis  <https://orcid.org/0000-0002-6624-4820>

## REFERENCES

- Allouche, O., Tsoar, A., & Kadmon, R. (2006). Assessing the accuracy of species distribution models: Prevalence, kappa and the true skill statistic (TSS). *Journal of Applied Ecology*, 43(6), 1223–1232. <https://doi.org/10.1111/j.1365-2664.2006.01214.x>
- Anderson, R. P., Martínez-Meyer, E., Nakamura, M., Araújo, M. B., Peterson, A. T., Soberón, J., & Pearson, R. G. (2011). Ecological niches and geographic distributions. In *Monographs in population biology*. Princeton University Press. <https://doi.org/10.1515/9781400840670>
- Anderson, R., Rand, A., Rothman, M., Share, A., & Bolton, J. (2007). Mapping and quantifying the South African kelp resource. *African Journal of Marine Science*, 29(3), 369–378. <https://doi.org/10.2989/AJMS.2007.29.3.5.335>
- Arafeh-Dalmau, N., Schoeman, D. S., Montaño-Moctezuma, G., Micheli, F., Rogers-Bennett, L., Olguín-Jacobson, C., & Possingham, H. P. (2020). Marine heat waves threaten kelp forests. *Science*, 367(6478), 635. <https://doi.org/10.1126/science.aba5244>
- Araújo, M. B., Anderson, R. P., Barbosa, A. M., Beale, C. M., Dormann, C. F., Early, R., Garcia, R. A., Guisan, A., Maiorano, L., Naimi, B., O'Hara, R. B., Zimmermann, N. E., & Rahbek, C. (2019). Standards for distribution models in biodiversity assessments. *Science Advances*, 5(1), 1–12. <https://doi.org/10.1126/sciadv.aat4858>
- Assis, J., Araújo, M. B., & Serrão, E. A. (2017). Projected climate changes threaten ancient refugia of kelp forests in the North Atlantic. *Global Change Biology*, 24(1), 1365–2486. <https://doi.org/10.1111/gcb.13818>

- Assis, J., Berecibar, E., Claro, B., Alberto, F., Reed, D., Raimondi, P., & Serrão, E. A. (2017). Major shifts at the range edge of marine forests: The combined effects of climate changes and limited dispersal. *Scientific Reports*, 7(1), 1–10. <https://doi.org/10.1038/srep44348>
- Assis, J., Fragkopoulou, E., Frade, D., Neiva, J., Oliveira, A., Abecasis, D., Faugeron, S., & Serrão, E. A. (2020). A fine-tuned global distribution dataset of marine forests. *Scientific Data*, 7(1), 119. <https://doi.org/10.1038/s41597-020-0459-x>
- Assis, J., Fragkopoulou, E., Serrão, E. A., Horta e Costa, B., Gandra, M., & Abecasis, D. (2021). Weak biodiversity connectivity in the European network of no-take marine protected areas. *Science of the Total Environment*, 773, 145664. <https://doi.org/10.1016/j.scitotenv.2021.145664>
- Assis, J., Serrão, E. A., Claro, B., Perrin, C., & Pearson, G. A. (2014). Climate-driven range shifts explain the distribution of extant gene pools and predict future loss of unique lineages in a marine brown alga. *Molecular Ecology*, 23(11), 2797–2810. <https://doi.org/10.1111/mec.12772>
- Assis, J., Tyberghein, L., Bosch, S., Verbruggen, H., Serrão, E. A., De Clerck, O., & Tittensor, D. (2017). Bio-ORACLE v2.0: Extending marine data layers for bioclimatic modelling. *Global Ecology and Biogeography*, 27(3), 277–284. <https://doi.org/10.1111/geb.12693>
- Ballesteros-Mejía, L., Kitching, I. J., Jetz, W., & Beck, J. (2017). Putting insects on the map: Near-global variation in sphingid moth richness along spatial and environmental gradients. *Ecography*, 40(6), 698–708. <https://doi.org/10.1111/ecog.02438>
- Barbet-Massin, M., Jiguet, F., Albert, C. H., & Thuiller, W. (2012). Selecting pseudo-absences for species distribution models: How, where and how many? *Methods in Ecology and Evolution*, 3(2), 327–338. <https://doi.org/10.1111/j.2041-210X.2011.00172.x>
- Barve, N., Barve, V., Jimenez-Valverde, A., Lira-Noriega, A., Maher, S. P., Peterson, A. T., Soberón, J., & Villalobos, F. (2011). The crucial role of the accessible area in ecological niche modeling and species distribution modeling. *Ecological Modelling*, 222(11), 1810–1819. <https://doi.org/10.1016/j.ecolmodel.2011.02.011>
- Bolton, J. J. (2010). The biogeography of kelps (Laminariales, Phaeophyceae): A global analysis with new insights from recent advances in molecular phylogenetics. *Helgoland Marine Research*, 64(4), 263–279. <https://doi.org/10.1007/s10152-010-0211-6>
- Bondaruk, B., Roberts, S. A., & Robertson, C. (2020). Discrete global grid systems: Operational capability of the current state of the art. *Geomatica*, 74(1), 9–30. <https://doi.org/10.1139/geomat-2019-0015>
- Bringloe, T. T., Starko, S., Wade, R. M., Vieira, C., Kawai, H., De Clerck, O., Cock, J. M., Coelho, S. M., Destombe, C., Valero, M., Neiva, J., Pearson, G. A., Faugeron, S., Serrão, E. A., & Verbruggen, H. (2020). Phylogeny and evolution of the brown algae. *Critical Reviews in Plant Sciences*, 39(4), 281–321. <https://doi.org/10.1080/0735689.2020.1787679>
- Bringloe, T. T., Verbruggen, H., & Saunders, G. W. (2020). Unique biodiversity in Arctic marine forests is shaped by diverse recolonization pathways and far northern glacial refugia. *Proceedings of the National Academy of Sciences of the United States of America*, 117(36), 22590–22596. <https://doi.org/10.1073/pnas.2002753117>
- Buschmann, A. H., Camus, C., Infante, J., Neori, A., Israel, Á., Hernández-González, M. C., Pereda, S. V., Gomez-Pinchetti, J. L., Golberg, A., Tadmor-Shalev, N., & Critchley, A. T. (2017). Seaweed production: Overview of the global state of exploitation, farming and emerging research activity. *European Journal of Phycology*, 52(4), 391–406. <https://doi.org/10.1080/09670262.2017.1365175>
- Cánovas, F. G., Mota, C. F., Serrão, E. A., & Pearson, G. A. (2011). Driving south: A multi-gene phylogeny of the brown algal family Fucaceae reveals relationships and recent drivers of a marine radiation. *BMC Evolutionary Biology*, 11(1), 371. <https://doi.org/10.1186/1471-2148-11-371>
- Cavanaugh, K. C., Reed, D. C., Bell, T. W., Castorani, M. C. N., & Beas-Luna, R. (2019). Spatial variability in the resistance and resilience of giant kelp in southern and Baja California to a multiyear heatwave. *Frontiers in Marine Science*, 6, 413. <https://doi.org/10.3389/fmars.2019.00413>
- Cavanaugh, K. C., Siegel, D. A., Reed, D. C., & Dennison, P. E. (2011). Environmental controls of giant-kelp biomass in the Santa Barbara Channel, California. *Marine Ecology Progress Series*, 429, 1–17. <https://doi.org/10.3354/meps09141>
- Chaudhary, C., Richardson, A. J., Schoeman, D. S., & Costello, M. J. (2021). Global warming is causing a pronounced dip in marine species richness at the equator. *Proceedings of the National Academy of Sciences of the United States of America*, 118(15), e2015094118. <https://doi.org/10.1073/pnas.2015094118>
- Chaudhary, C., Saeedi, H., & Costello, M. J. (2016). Bimodality of latitudinal gradients in marine species richness. *Trends in Ecology & Evolution*, 31(9), 670–676. <https://doi.org/10.1016/j.tree.2016.06.001>
- Coleman, M. A., & Wernberg, T. (2017). Forgotten underwater forests: The key role of fucoids on Australian temperate reefs. *Ecology and Evolution*, 7(20), 8406–8418. <https://doi.org/10.1002/ece3.3279>
- Cooper, J. C., & Soberón, J. (2018). Creating individual accessible area hypotheses improves stacked species distribution model performance. *Global Ecology and Biogeography*, 27(1), 156–165. <https://doi.org/10.1111/geb.12678>
- Costello, M. J., Coll, M., Danovaro, R., Halpin, P., Ojaveer, H., & Miloslavich, P. (2010). A census of marine biodiversity knowledge, resources and future challenges. *PLoS One*, 5(8), e12110. <https://doi.org/10.1371/journal.pone.0012110>
- Costello, M. J., Tsai, P., Wong, P. S., Cheung, A. K. L., Basher, Z., & Chaudhary, C. (2017). Marine biogeographic realms and species endemicity. *Nature Communications*, 8(1), 1–9. <https://doi.org/10.1038/s41467-017-01121-2>
- Coyer, J. A., Hoarau, G., Oudot-Le Secq, M. P., Stam, W. T., & Olsen, J. L. (2006). A mtDNA-based phylogeny of the brown algal genus *Fucus* (Heterokontophyta; Phaeophyta). *Molecular Phylogenetics and Evolution*, 39(1), 209–222. <https://doi.org/10.1016/j.ympev.2006.01.019>
- Crisp, M. D., Laffan, S., Linder, H. P., & Monroe, A. (2001). Endemism in the Australian flora. *Journal of Biogeography*, 28(2), 183–198. <https://doi.org/10.1046/j.1365-2699.2001.00524.x>
- De'ath, G. (2007). Boosted trees for ecological modelling and prediction. *Ecology*, 88(1), 243–251.
- Dormann, C. F., Elith, J., Bacher, S., Buchmann, C., Carl, G., Carré, G., Marquéz, J. R. G., Gruber, B., Lafourcade, B., Leitão, P. J., Mürkemüller, T., McClean, C., Osborne, P. E., Reineking, B., Schröder, B., Skidmore, A. K., Zurell, D., & Lautenbach, S. (2013). Collinearity: A review of methods to deal with it and a simulation study evaluating their performance. *Ecography*, 36(1), 27–46. <https://doi.org/10.1111/j.1600-0587.2012.07348.x>
- Dormann, C. M., McPherson, J. M., Araújo, M. B., Bivand, R., Bolliger, J., Carl, G., Davies, R. G., Hirzel, A., Jetz, W., Kissling, W. D., Kühn, I., Ohlemüller, R., Peres-Neto, P. R., Reineking, B., Schröder, B., Schurr, F. M., & Wilson, R. (2007). Methods to account for spatial autocorrelation in the analysis of species distributional data: A review. *Ecography*, 30(5), 609–628. <https://doi.org/10.1111/j.2007.0906-7590.05171.x>
- Elith, J., Graham, C. H., Anderson, R. P., Dudík, M., Ferrier, S., Guisan, A., Hijmans, R. J., Huettmann, F., Leathwick, J. R., Lehmann, A., Li, J., Lohmann, L. G., Loiselle, B. A., Manion, G., Moritz, C., Nakamura, M., Nakazawa, Y., Overton, J., McC. M., Townsend Peterson, A., ... Zimmermann, N. E. (2006). Novel methods improve prediction of species' distributions from occurrence data. *Ecography*, 29(2), 129–151. <https://doi.org/10.1111/j.2006.0906-7590.04596.x>
- Elith, J., Leathwick, J. R., & Hastie, T. (2008). A working guide to boosted regression trees. *Journal of Animal Ecology*, 77(4), 802–813. <https://doi.org/10.1111/j.1365-2656.2008.01390.x>

- Fairley, I., Lewis, M., Robertson, B., Hemer, M., Masters, I., Horrillo-Caraballo, J., Karunarathna, H., & Reeve, D. E. (2020). A classification system for global wave energy resources based on multivariate clustering. *Applied Energy*, 262, 114515. <https://doi.org/10.1016/j.apenergy.2020.114515>
- Fielding, A. H., & Bell, J. F. (1997). A review of methods for the assessment of prediction errors in conservation presence/absence models. *Environmental Conservation*, 24(1), 38–49. <https://doi.org/10.1017/S0376892997000088>
- Fragkopoulou, E., Serrão, E. A., Horta, P. A., Koerich, G., & Assis, J. (2021). Bottom trawling threatens future climate refugia of rhodoliths globally. *Frontiers in Marine Science*, 7, 594537. <https://doi.org/10.3389/fmars.2020.594537>
- Gagné, T. O., Reygondeau, G., Jenkins, C. N., Sexton, J. O., Bograd, S. J., Hazen, E. L., & van Houtan, K. S. (2020). Towards a global understanding of the drivers of marine and terrestrial biodiversity. *PLoS One*, 15(2), e0228065. <https://doi.org/10.1371/journal.pone.0228065>
- García-Callejas, D., & Araújo, M. B. (2016). Model and data complexity on predictions from species distributions models. *Ecological Modelling*, 326, 4–12. <https://doi.org/10.1016/j.ecolmodel.2015.06.002>
- Gouvêa, L. P., Assis, J., Gurgel, C. F. D., Serrão, E. A., Silveira, T. C. L., Santos, R., Duarte, C. M., Peres, L. M. C., Carvalho, V. F., Batista, M., Bastos, E., Sissini, M. N., & Horta, P. A. (2020). Golden carbon of *Sargassum* forests revealed as an opportunity for climate change mitigation. *Science of the Total Environment*, 729, 138741. <https://doi.org/10.1016/j.scitotenv.2020.138745>
- Guiry, M. D., & Guiry, G. M. (2021, September 24). AlgaeBase. National University of Ireland. <https://www.algaebase.org>
- Guisan, A., & Rahbek, C. (2011). SESAM—A new framework integrating macroecological and species distribution models for predicting spatio-temporal patterns of species assemblages. *Journal of Biogeography*, 38(8), 1433–1444. <https://doi.org/10.1111/j.1365-2699.2011.02550.x>
- Gurgel, C. F. D., Camacho, O., Minne, A. J. P., Wernberg, T., & Coleman, M. A. (2020). Marine heatwave drives cryptic loss of genetic diversity in underwater forests. *Current Biology*, 30(7), 1199–1206.e2. <https://doi.org/10.1016/j.cub.2020.01.051>
- Harisena, N. V., Groen, T. A., Toxopeus, A. G., & Naimi, B. (2021). When is variable importance estimation in species distribution modelling affected by spatial correlation? *Ecography*, 44(5), 1–11. <https://doi.org/10.1111/ecog.05534>
- Harrison, S., & Noss, R. (2017). Endemism hotspots are linked to stable climatic refugia. *Annals of Botany*, 119(2), 207–214. <https://doi.org/10.1093/aob/mcw248>
- Hofner, B., Müller, J., & Hothorn, T. (2011). Monotonicity-constrained species distribution models. *Ecology*, 92(10), 1895–1901. <https://doi.org/10.1890/10-2276.1>
- Horton, T., Kroh, A., Ahyong, S., Bailly, N., Bieler, R., Boyko, C. B., Brandão, S. N., Gofas, S., Hooper, J. N. A., Hernandez, F., Mees, J., Molodtsova, T. N., Paulay, G., Bouirig, K., Decock, W., Dekeyzer, S., Vandepitte, L., Vanhoorne, B., Adlard, R., ... Zhao, Z. (2021). World Register of Marine Species. <http://www.marinespecies.org>
- IPCC. (2021). Chapter 4: Future Global Climate: Scenario-Based Projections and Near-Term Information. In J.-Y. Lee, J. Marotzke, G. Bala, L. Cao, S. Corti, J. P. Dunne, F. Engelbrecht, E. Fischer, J. C. Fyfe, C. Jones, A. Maycock, J. Mutemi, O. Ndiaye, S. Panical, & T. Zhou (Eds.), *Climate change 2021: The physical science basis. Contribution of Working Group I to the Sixth Assessment Report of the Intergovernmental Panel on Climate Change* [V. Masson-Delmotte, P. Zhai, A. Pirani, S. L. Connors, C. Péan, S. Berger, N. Caud, Y. Chen, L. Goldfarb, M. I. Gomis, M. Huang, K. Leitzell, E. Lonnoy, J. B. R. Matthews, T. K. Maycock, T. Waterfield, O. Yelekçi, R. Yu, & B. Zhou (Eds.)]. Cambridge University Press. In Press.
- Jayathilake, D. R. M., & Costello, M. J. (2020). A modelled global distribution of the kelp biome. *Biological Conservation*, 252, 108815. <https://doi.org/10.1016/j.biocon.2020.108815>
- Jayathilake, D. R. M., & Costello, M. J. (2021). Version 2 of the world map of laminarian kelp benefits from more Arctic data and makes it the largest marine biome. *Biological Conservation*, 257, 109099. <https://doi.org/10.1016/j.biocon.2021.109099>
- Keith, S. A., Kerswell, A. P., & Connolly, S. R. (2014). Global diversity of marine macroalgae: Environmental conditions explain less variation in the tropics. *Global Ecology and Biogeography*, 23(5), 517–529. <https://doi.org/10.1111/geb.12132>
- Kerswell, A. P. (2006). Global biodiversity patterns of benthic marine algae. *Ecology*, 87(10), 2479–2488.
- Krause-Jensen, D., Lavery, P., Serrano, O., Marba, N., Masque, P., & Duarte, C. M. (2018). Sequestration of macroalgal carbon: The elephant in the Blue Carbon room. *Biology Letters*, 14(6), 20180236. <https://doi.org/10.1098/rsbl.2018.0236>
- Krause-Jensen, D., Marbà, N., Olesen, B., Sejr, M. K., Christensen, P. B., Rodrigues, J., Renaud, P. E., Balsby, T. J. S., & Rysgaard, S. (2012). Seasonal sea ice cover as principal driver of spatial and temporal variation in depth extension and annual production of kelp in Greenland. *Global Change Biology*, 18(10), 2981–2994. <https://doi.org/10.1111/j.1365-2486.2012.02765.x>
- Kusumoto, B., Costello, M. J., Kubota, Y., Shiono, T., Wei, C. L., Yasuhara, M., & Chao, A. (2020). Global distribution of coral diversity: Biodiversity knowledge gradients related to spatial resolution. *Ecological Research*, 35(2), 315–326. <https://doi.org/10.1111/1440-1703.12096>
- Lourenço, C. R., Zardi, G. I., McQuaid, C. D., Serrão, E. A., Pearson, G. A., Jacinto, R., & Nicastro, K. R. (2016). Upwelling areas as climate change refugia for the distribution and genetic diversity of a marine macroalga. *Journal of Biogeography*, 43(8), 1595–1607. <https://doi.org/10.1111/jbi.12744>
- Martins, M. R., Assis, J., & Abecasis, D. (2021). Biologically meaningful distribution models highlight the benefits of the Paris Agreement for demersal fishing targets in the North Atlantic Ocean. *Global Ecology and Biogeography*, 30(8), 1643–1656. <https://doi.org/10.1111/geb.13327>
- Mendes, P., Velazco, S. J. E., de Andrade, A. F. A., & De Marco, P. (2020). Dealing with overprediction in species distribution models: How adding distance constraints can improve model accuracy. *Ecological Modelling*, 431, 109180. <https://doi.org/10.1016/j.ecolmodel.2020.109180>
- Nicastro, K. R., Zardi, G. I., Teixeira, S., Neiva, J., Serrão, E. A., & Pearson, G. A. (2013). Shift happens: Trailing edge contraction associated with recent warming trends threatens a distinct genetic lineage in the marine macroalga *Fucus vesiculosus*. *BMC Biology*, 11, 6. <https://doi.org/10.1186/1741-7007-11-6>
- Pecl, G. T., Araújo, M. B., Bell, J. D., Blanchard, J., Bonebrake, T. C., Chen, I.-C., Clark, T. D., Colwell, R. K., Danielsen, F., Evengård, B., Falconi, L., Ferrier, S., Frusher, S., Garcia, R. A., Griffis, R. B., Hobday, A. J., Janion-Scheepers, C., Jarzyna, M. A., Jennings, S., ... Williams, S. E. (2017). Biodiversity redistribution under climate change: Impacts on ecosystems and human well-being. *Science*, 355(6332), eaai9214. <https://doi.org/10.1126/science.aai9214>
- Peters, A. F., Oppen, M. J. H., Wiencke, C., Stam, W. T., & Olsen, J. L. (1997). Phylogeny and historical ecology of the Desmarestiaceae (Phaeophyceae) support a Southern Hemisphere origin. *Journal of Phycology*, 33(2), 294–309. <https://doi.org/10.1111/j.0022-3646.1997.00294.x>
- R Development Core Team. (2021). *A language and environment for statistical computing*. R Foundation for Statistical Computing. <https://www.R-project.org>
- Randin, C. F., Dirnböck, T., Dullinger, S., Zimmermann, N. E., Zappa, M., & Guisan, A. (2006). Are niche-based species distribution models

- transferable in space? *Journal of Biogeography*, 33(10), 1689–1703. <https://doi.org/10.1111/j.1365-2699.2006.01466.x>
- Schmitt, S., Pouteau, R., Justeau, D., de Boissieu, F., & Birnbaum, P. (2017). ssdm: An r package to predict distribution of species richness and composition based on stacked species distribution models. *Methods in Ecology and Evolution*, 8(12), 1795–1803. <https://doi.org/10.1111/2041-210X.12841>
- Schubert, H., Feuerpfeil, P., Marquardt, R., Telesh, I., & Skarlato, S. (2011). Macroalgal diversity along the Baltic Sea salinity gradient challenges Remane's species-minimum concept. *Marine Pollution Bulletin*, 62(9), 1948–1956. <https://doi.org/10.1016/j.marpolbul.2011.06.033>
- Selig, E. R., Turner, W. R., Troëng, S., Wallace, B. P., Halpern, B. S., Kaschner, K., Lascelles, B. G., Carpenter, K. E., & Mittermeier, R. A. (2014). Global priorities for marine biodiversity conservation. *PLoS One*, 9(1), e82898. <https://doi.org/10.1371/journal.pone.0082898>
- Sequeira, A. M. M., Bouchet, P. J., Yates, K. L., Mengersen, K., & Caley, M. J. (2018). Transferring biodiversity models for conservation: Opportunities and challenges. *Methods in Ecology and Evolution*, 9(5), 1250–1264. <https://doi.org/10.1111/2041-210X.12998>
- Serrão, E. A., Alice, L. A., & Brawley, S. H. (1999). Evolution of the Fucaceae (Phaeophyceae) inferred from nrDNA-ITS. *Journal of Phycology*, 35(2), 382–394. <https://doi.org/10.1046/j.1529-8817.1999.3520382.x>
- Spalding, M. D., Fox, H. E., Allen, G. R., Davidson, N., Ferdaña, Z. A., Finlayson, M., Halpern, B. S., Jorge, M. A., Lombana, A., Lourie, S. A., Martin, K. D., McManus, E., Molnar, J., Recchia, C. A., & Robertson, J. (2007). Marine Ecoregions of the World: A bioregionalization of coastal and shelf areas. *BioScience*, 57(7), 573–583. <https://doi.org/10.1641/B570707>
- Starko, S., Soto Gomez, M., Darby, H., Demes, K. W., Kawai, H., Yotsukura, N., Lindstrom, S. C., Keeling, P. J., Graham, S. W., & Martone, P. T. (2019). A comprehensive kelp phylogeny sheds light on the evolution of an ecosystem. *Molecular Phylogenetics and Evolution*, 136, 138–150. <https://doi.org/10.1016/j.ympev.2019.04.012>
- Taheri, S., Naimi, B., Rahbek, C., & Araújo, M. B. (2021). Improvements in reports of species redistribution under climate change are required. *Science Advances*, 7(15), eabe1110. <https://doi.org/10.1126/sciadv.abe1110>
- Thuiller, W., Brotons, L., Araújo, M. B., & Lavorel, S. (2004). Effects of restricting environmental range of data to project current and future species distributions. *Ecography*, 27(2), 165–172. <https://doi.org/10.1111/j.0906-7590.2004.03673.x>
- Tittensor, D. P., Mora, C., Jetz, W., Lotze, H. K., Ricard, D., Berghe, E. V., & Worm, B. (2010). Global patterns and predictors of marine biodiversity across taxa. *Nature*, 466(7310), 1098–1101. <https://doi.org/10.1038/nature09329>
- Trebilco, R., Halpern, B. S., Mills, J., Field, C., Blanchard, W., & Worm, B. (2011). Mapping species richness and human impact drivers to inform global pelagic conservation prioritisation. *Biological Conservation*, 144(5), 1758–1766. <https://doi.org/10.1016/j.biocon.2011.02.024>
- Tyberghein, L., Verbruggen, H., Pauly, K., Troupin, C., Mineur, F., & De Clerck, O. (2012). Bio-ORACLE: A global environmental dataset for marine species distribution modelling. *Global Ecology and Biogeography*, 21(2), 272–281. <https://doi.org/10.1111/j.1466-8238.2011.00656.x>
- van Proosdij, A. S. J., Sosef, M. S. M., Wieringa, J. J., & Raes, N. (2016). Minimum required number of specimen records to develop accurate species distribution models. *Ecography*, 39(6), 542–552. <https://doi.org/10.1111/ecog.01509>
- Verbruggen, H., Tyberghein, L., Pauly, K., Vlaeminck, C., Nieuwenhuyze, K. V., Kooistra, W. H. C. F., Leliaert, F., & de Clerck, O. (2009). Macroecology meets macroevolution: Evolutionary niche dynamics in the seaweed *Halimeda*. *Global Ecology and Biogeography*, 18(4), 393–405. <https://doi.org/10.1111/j.1466-8238.2009.00463.x>
- Vieira, C., Steen, F., D'hondt, S., Bafort, Q., Tyberghein, L., Fernandez-García, C., Wyssor, B., Tronholm, A., Mattio, L., Payri, C., Kawai, H., Saunders, G., Leliaert, F., Verbruggen, H., & De Clerck, O. (2021). Global biogeography and diversification of a group of brown seaweeds (Phaeophyceae) driven by clade-specific evolutionary processes. *Journal of Biogeography*, 48(4), 703–715. <https://doi.org/10.1111/jbi.14047>
- Vignal, S., Barras, A. G., Arlettaz, R., & Braunisch, V. (2020). SDMtune: An R package to tune and evaluate species distribution models. *Ecology and Evolution*, 10(20), 11488–11506. <https://doi.org/10.1002/ece3.6786>
- Wernberg, T., Krumhansl, K., Filbee-Dexter, K., & Pedersen, M. F. (2019). Status and trends for the world's kelp forests. In C. Sheppard (Ed.), *World seas: An environmental evaluation* (2nd ed., pp. 57–78). Elsevier. <https://doi.org/10.1016/B978-0-12-805052-1.00003-6>
- Wernberg, T., Smale, D. A., Tuya, F., Thomsen, M. S., Langlois, T. J., De Bettignies, T., Bennett, S., & Rousseaux, C. S. (2013). An extreme climatic event alters marine ecosystem structure in a global biodiversity hotspot. *Nature Climate Change*, 3(1), 78–82. <https://doi.org/10.1038/nclimate1627>
- Wiens, J. J., & Donoghue, M. J. (2004). Historical biogeography, ecology and species richness. *Trends in Ecology & Evolution*, 19(12), 639–644. <https://doi.org/10.1016/j.tree.2004.09.011>
- Wilson, K. L., Skinner, M. A., & Lotze, H. K. (2019). Projected 21st-century distribution of canopy-forming seaweeds in the Northwest Atlantic with climate change. *Diversity and Distributions*, 25(4), 582–602. <https://doi.org/10.1111/ddi.12897>
- Yip, Z. T., Quek, R. Z. B., & Huang, D. (2020). Historical biogeography of the widespread macroalgae *Sargassum* (Fucales, Phaeophyceae). *Journal of Phycology*, 56(2), 300–309. <https://doi.org/10.1111/jpy.12945>
- Zhao, Q., Stephenson, F., Lundquist, C., Kaschner, K., Jayathilake, D., & Costello, M. J. (2020). Where Marine Protected Areas would best represent 30% of ocean biodiversity. *Biological Conservation*, 244, 108536. <https://doi.org/10.1016/j.biocon.2020.108536>

## BIOSKETCH

**Eliza Fragkopoulou** (junior researcher) is based at CCMAR, University of the Algarve, Portugal. Her research is focused on species distribution modelling, past and future climate-driven range shifts, landscape genetics at multiple temporal and spatial scales and putative climate/genetic refugia of marine forest species at global scales, in the scope of conservation management.

## SUPPORTING INFORMATION

Additional supporting information may be found in the online version of the article at the publisher's website.

**How to cite this article:** Fragkopoulou, E., Serrão E. A., De Clerck O., Costello M. J., Araújo M. B., Duarte C. M., Krause-Jensen D., & Assis J. (2021). Global biodiversity patterns of marine forests of brown macroalgae. *Global Ecology and Biogeography*, 00, 1–13. <https://doi.org/10.1111/geb.13450>